Research Square

Preprints are preliminary reports that have not undergone peer review.
They should not be considered conclusive, used to inform clinical practice,
or referenced by the media as validated information.

Ditch-buried straw return enhanced maize growth via improving soil physicochemical and microbial properties in soda saline-alkali soils

Xuan Chen
Nanjing Agricultural University
Paidamoyo N Mataranyika
Imperial College London
Zhe Liu
Nanjing Agricultural University
Tingting Li
Shenyang Research Institute of Chemical Industry (China)
Pai Peng
Shenyang Research Institute of Chemical Industry (China)
Xiaona Wei
Liaoning Petrochemical University
Hongjun Liu
Nanjing Agricultural University
Zhipeng Liu
Nanjing Agricultural University
Zongzhuan Shen
shenzongz@njau.edu.cn
Nanjing Agricultural University
Weiyu Shi
Southwest University
Rong Li
Nanjing Agricultural University

Research Article

Keywords: Ditch-buried straw return, Soda saline-alkali soils, Soil conditions, Maize growth, Bacterial communities, Spatial heterogeneity

Posted Date: November 13th, 2026

DOI: https://doi.org/10.21203/rs.3.rs-11499799/v1

License: This work is licensed under a Creative Commons Attribution 4.0 International License.
Read Full License

Additional Declarations: No competing interests reported.

Abstract

Ditch-buried straw return (DB-SR) is a promising practice for improving saline-alkali soils. However, the underlying mechanisms of DB-SR on improving saline-alkali soils remain not fully understood. We conducted a field experiment in a typical soda saline-alkali maize field in China with three sampling zones, including the ditch zone (SD), near-ditch zone (SN), and far-ditch zone (SF), along a horizontal gradient from the centerline of the straw-filled ditch. Soil physicochemical and microbial properties in bulk and rhizosphere soils characterized by 16S rRNA gene amplicon sequencing, were determined in the present study. Our results showed spatial heterogeneity under DB-SR, i.e., soil pH was lower, but electrical conductivity (EC) was higher in SN and SF than in SD, whereas maize growth generally increased from SD to SF. Although bacterial alpha diversity did not differ significantly among treatments, community composition varied significantly across the gradient in bulk soil but not in rhizosphere soil. Several differentially abundant ASVs, belonging to *Clostridium*, *Phyllobacterium*, and *Niabella*, were significantly correlated with shoot biomass. Our findings suggest that DB-SR provides a ditch-centered spatially heterogeneous environment, improves local soil conditions in zones adjacent to the straw-filled ditch, and may contribute to enhanced maize growth, partly through manipulating bacterial community composition.

1 Introduction

The reclamation and sustainable utilization of saline-alkali soils is always a major challenge for sustainable agriculture worldwide (Tarolli et al., 2024). Soda saline-alkali soil, a typical saline-alkali soil, presents a particular challenge for development and utilization due to the elevated pH, high salinity, and poor physical structure, all of which severely restrict crop growth and agricultural productivity (Wang et al., 2024; Shan et al., 2026; Yu et al., 2010). Straw return is generally considered to be an effective agronomic practice for improving soil fertility, increasing soil organic matter, and shaping soil microbial communities (Pan et al., 2022). Among various straw-return methods, ditch-buried straw return (DB-SR) has recently been developed by placing crop straw into excavated subsurface ditches within the soil profile to loosen compacted subsurface layers and facilitate straw incorporation into deeper soil layers, potentially improving subsoil fertility and physical conditions (Dou, 2019). DB-SR has been shown to enhance subsoil organic carbon sequestration and increase crop yield, highlighting its potential as an effective subsoil management strategy (Kan et al., 2025). Hence, DB-SR is emerging as a promising management strategy for improving local soil conditions and supporting crop growth in saline-alkali farmlands.

Recent research on DB-SR has predominantly focused on the paddy system, where positive effects on soil conditions and crop yields have been documented (Kan et al., 2025). Because straw, under DB-SR, is incorporated into concentrated subsurface ditches, its impacts may vary between the ditch zone and the surrounding soil matrix. This spatial heterogeneity may be particularly pronounced in soda saline-alkali soils, where concurrent stresses, including high salinity, elevated pH, and limited nutrient availability, can intensify localized variations in soil processes and agronomic performance (Rengasamy, 2010).

Consequently, elucidating this spatial heterogeneity and its subsequent effects on localized soil properties, bacterial communities and maize growth indicators can provide proof of viability of DB-SR as an agricultural management strategy in soda saline-alkali farmlands. However, the specific mechanisms through which DB-SR modulates soda saline-alkali soils along this ditch-centered spatial gradient remain insufficiently understood. Although DB-SR has demonstrated potential to enhance soil quality and crop productivity in certain cropping systems, its efficacy within soda saline-alkali maize fields has yet to be fully clarified.

It is widely accepted that soil microorganisms, especially bacteria, are key drivers of straw decomposition and nutrient cycling (Wu et al., 2019; Tang et al., 2018; Zhao et al., 2023). The microscale environmental gradients generated by deep buried straw return (DB-SR) are highly inferred to reshape bacterial community composition and co-occurrence patterns along the ditch-soil continuum. Nevertheless, current research on straw return has predominantly focused on systemic changes in soil physicochemical properties or overall microbial community structure (Ninkuu et al., 2025; Wu et al., 2025). However, the effects and mechanisms of localized heterogeneity induced by concentrated straw incorporation on specific bacterial taxa and their co-occurrence relationships along ditch-centered spatial gradient are still largely unknown. Consequently, a comprehensive understanding of how bacterial communities respond to this spatial heterogeneity within soda saline-alkali farmlands is extremely crucial and urgent.

In this study, we sought to systematically explore the effects of DB-SR on both soil physicochemical and microbial properties in soda saline-alkali soils. To achieve this, a field experiment was conducted in a typical soda saline-alkali maize field managed under ditch-buried straw return (DB-SR). Three sampling zones: the ditch zone (SD), the near-ditch zone (SN), and the far-ditch zone (SF) were prepared along a horizontal distance gradient extending from the centerline of the straw-filled ditch for investigation. We hypothesized that DB-SR would establish a ditch-centered spatial gradient in soil physicochemical properties, thereby ameliorating localized soil conditions within specific zones, concurrently stimulating maize growth and modulating bacterial community structures. The present study aims to 1) explore the responses of soil physicochemical properties and maize growth across the ditch-centered spatial gradient under DB-SR, 2) reveal the variations in bacterial community composition and differential taxa within both bulk and rhizosphere soils along this gradient, and 3) decipher the structural disparities in bacterial co-occurrence networks among the different sampling zones and between soil compartments. Ultimately, this study provides a spatial ecological perspective for understanding the mechanisms of DB-SR in soda saline-alkali farmlands and offers a scientific foundation for optimizing its application in analogous agricultural systems.

2 Material and method

2.1 Field experiment description

The field experiment was conducted in Zhenlai County, a part of western Songnen Plain and a typical soda saline-alkali soil region, located in Baicheng City, Jilin Province, China (46°06'N, 123°03'E). In May 2024, ditches 30 cm wide and 50 cm deep were excavated and filled with chopped maize straw, and then covered with a 5-cm topsoil layer as shown in Fig. 1. The straw used for ditch burial was collected from the preceding maize crop grown in the experimental field with permission from the landowner, air-dried and stored before incorporation, and chopped into short fragments before being placed into the ditches. The straw-filled ditches were arranged in a 10 m × 10 m grid pattern across the experimental field. Organic fertilizer, gypsum, and a citric acid-based amendment for straw decomposition were uniformly broadcast across the entire experimental field before sowing as basal amendments at rates of 60, 60, and 15 t ha^{-1}, respectively. Maize (*Zea mays* L.) cultivar 'Tianyu 108', a commonly grown local maize cultivar, was commercially purchased from Jilin Yuntianhua Seed Industry Technology Co., Ltd., China, and mechanically sown in late April 2025. The field experiment and collection of soil and maize samples were conducted with permission from the landowner. Ridges were spaced 1.2 m apart, with two maize rows on each ridge and an intra-row plant spacing of 23 cm, corresponding to an approximate planting density of 7.2×10^4 plants ha^{-1}. Irrigation and other agronomic practices were managed uniformly across the experimental field according to local practice. Soil and plant samples were collected on July 31, 2025, approximately 14 months after straw burial in the ditches and three months after maize was sown. Three further sampling sites were established at 30-m intervals along a selected straw-filled ditch. At each sampling site, three subsampling zones including the ditch zone (SD), the near-ditch zone (SN), and the far-ditch zone (SF) were defined according to horizontal distance from the ditch centerline (Fig. 1a). In detail, the ditch zone (SD) represents soil samples which were collected from the center of the refilled ditch while the near-ditch zone (SN) refers to soil samples which were collected from within 1.0 m of the ditch centerline but outside the refilled ditch. The far-ditch zone (SF) indicated samples that were collected from soil located 1.0–2.0 m from the ditch centerline.

2.2 Plant biomass measurement and soil sample collection

At the pre-tasseling stage of maize, three plants were randomly selected for plant and soil collection from each of the three subsampling zones (SD, SN, and SF) at each sampling site. For all zones, soil samples were collected from the 0–20 cm soil layer using the same sampling depth. Rhizosphere soil was obtained from roots collected within the same 0–20 cm soil layer. Plant height and stem diameter were measured *in situ*. Plant height was measured from the soil surface to the tip of the uppermost leaf using a ruler. Stem diameter was measured at the third internode above the plant base using a vernier caliper. Following this, shoots were harvested, and their fresh weight was recorded. To determine shoot dry weight, shoot samples were initially dried at 105°C for 30 min and then oven-dried at 65°C to constant weight. For plant growth analyses, measurements from all sampled plants were treated as individual observations, yielding nine plant-level samples for each zone (SD, SN, and SF, three sampling sites × three plants per site).

Soil loosely adhered to the roots was shaken and collected as bulk soil after the root system of each sampled plant was gently removed by hand. After passing through a 2-mm sieve, the bulk soil samples were divided into two parts. In detail, one part was stored at -80°C for DNA extraction, and the other was air-dried for determination of soil physicochemical properties. For soil physicochemical analyses, each bulk soil sample associated with an individual plant was analyzed separately, yielding nine bulk soil samples for each zone. Roots with tightly adhering rhizosphere soil were cut into 1.0 cm segments and added into Erlenmeyer flasks previously loaded with sterile distilled water. The flasks were shaken at 180 rpm for 30 min to detach rhizosphere soil from the root surface and obtain a soil suspension. The suspension was then centrifuged at 8000 rpm for 15 min at 4°C to collect rhizosphere soil pellets for analysis. Each plant-associated bulk and rhizosphere soil sample was treated as an individual sample for microbial community analysis.

2.3 Soil physicochemical properties determination

Soil basic physicochemical properties, including soil pH, organic matter (OM), electrical conductivity (EC), alkali-hydrolysable nitrogen (AHN), total nitrogen (TN), available phosphorus (AP), and available potassium (AK) were determined according to the previously described method (Cao et al., 2024). In brief, soil pH and electrical conductivity (EC) were done on the 1:5 (w/v) soil-to-water suspension by using pH meter and EC meter. AHN was determined using the alkaline hydrolysis diffusion method while TN was measured by the Kjeldahl method. AK was determined by ammonium acetate extraction followed by flame photometry, whereas AP was determined by the quinolinium phosphomolybdate colorimetric method. OM was determined by the potassium dichromate oxidation method with external heating.

2.4 DNA extraction, PCR amplification, and sequencing

Total soil genomic DNA was extracted from approximately 0.5 g of each bulk and rhizosphere soil sample by using the DNeasy® PowerSoil® Pro Kit (Qiagen, Hilden, Germany) following manufacturer protocols. DNA quality and concentration were verified using the NanoDrop 2000 spectrophotometry and used as sequencing templates. Sequencing libraries were constructed following the method described by Caporaso et al. (2011). The V4 hypervariable region of the bacterial 16S rRNA gene was amplified using the forward primer 515F (5'-GTGCCAGCMGCCGCGGTAA-3') and the reverse primer 806R (5'-GGACTACHVGGGTWTCTAAT-3'). PCR amplification, library construction, and Illumina MiSeq PE 250 sequencing were performed at MAGIGENE Co., Ltd., China, according to their standard pipeline. All raw sequence data have been deposited in the NCBI Sequence Read Archive database under the accession number PRJNA1490355.

2.5 Sequence processing and bioinformatic analysis

Raw paired-end 16S rRNA gene sequences were processed using QIIME2 v2024.5. Quality filtering, denoising, paired-end read merging, and chimera removal were performed using DADA2 to generate amplicon sequence variants (ASVs) (Callahan et al., 2016). Based on sequence quality profiles, the first 19 bp of the forward reads and 20 bp of the reverse reads were trimmed from the 5' ends, and the reads

were truncated at 240 bp and 230 bp, respectively. Taxonomic assignment was performed using a naive Bayes classifier trained on the 16S rRNA gene V4 region extracted from the Greengenes 13.8 database (Werner *et al.*, 2012). Non-bacterial sequences, as well as chloroplast- and mitochondria-associated sequences, were removed prior to downstream analyses. All samples were rarefied to 10,000 sequences per sample prior to diversity analysis.

After rarefaction, alpha- and beta-diversity metrics, including Shannon diversity and Bray-Curtis dissimilarity, were calculated in QIIME2. Beta diversity was visualized by non-metric multidimensional scaling (NMDS) based on Bray-Curtis dissimilarity. Differences in bacterial community composition among sampling zones were tested separately for bulk and rhizosphere soils using PERMANOVA based on Bray-Curtis dissimilarity with 999 permutations. Taxonomic composition at the phylum level was visualized using stacked bar plots showing the top 10 most abundant phyla, with the remaining phyla grouped into “others”.

Key ASVs among sampling zones were identified separately for bulk and rhizosphere soils by using the ‘edgeR’ package in R v4.4.2 (Robinson et al., 2010). Low-abundance ASVs were firstly filtered by using a mean relative abundance threshold of 0.01%. Then pairwise comparisons including SD/SF, SN/SF, and SD/SN were performed while ASVs with a false discovery rate (FDR) < 0.05 and $|\log_2$ fold change$| > 1$ were considered to be significantly differed among treatments. Differential ASVs were visualized using volcano plots. ASVs significantly enriched in each sampling zone across relevant pairwise comparisons were pooled into zone-specific sets, and overlaps among these sets were visualized using Venn diagrams.

For each soil compartment, the top 15 enriched ASVs ranked by overall abundance were selected from the zone-enriched ASV sets, and their $\log_2$ fold changes in the SD/SF and SN/SF comparisons were visualized using bar plots. These selected ASVs were further used for Spearman’s rank correlation analysis with plant growth traits, including plant height, stem diameter, shoot fresh weight, and shoot dry weight. Correlation coefficients and significance levels were visualized and plotted using heatmaps in R v4.4.2.

2.6 Co-occurrence network analysis

Co-occurrence networks were constructed and visualized in Gephi v0.9.2 separately for each soil compartment and sampling zone based on ASV abundance data (Yuan et al., 2025; Bastian et al., 2009). Within each group, ASVs detected in all nine biological replicates were retained as core ASVs, and pairwise associations among these ASVs were calculated using Spearman’s rank correlation. Correlations with $|\rho| \geq 0.85$ and $P < 0.05$ were used to construct undirected co-occurrence networks using the ‘igraph’ and ‘WGCNA’ packages in R v4.4.2 (Csardi and Nepusz, 2006; Langfelder and Horvath, 2008). Topological properties of the networks, including the proportion of positive correlations, modularity, and global efficiency, were calculated in R v4.4.2. Node topological roles were classified according to the Zi–Pi framework, where nodes with $Zi \leq 2.5$ and $Pi \leq 0.62$ were defined as peripherals,

nodes with Zi ≤ 2.5 and Pi > 0.62 as connectors, nodes with Zi > 2.5 and Pi ≤ 0.62 as module hubs, and nodes with Zi > 2.5 and Pi > 0.62 as network hubs.

2.7 Statistical analysis

Soil physicochemical properties, plant growth traits, and Shannon diversity index were compared among sampling zones using one-way analysis of variance (ANOVA), followed by Tukey's HSD test, with significance determined at $P < 0.05$. These analyses were conducted separately for bulk and rhizosphere soils where applicable. Phylum-level relative abundances were also compared among sampling zones using one-way ANOVA followed by Tukey's HSD test, with significance determined at $P < 0.05$. Redundancy analysis (RDA) was performed using the 'vegan' package in R v4.4.2 to evaluate relationships between bulk soil bacterial community composition and environmental variables. In short, the ASV abundance table was Hellinger-transformed prior to RDA and all measured soil variables were initially included in the RDA. After variance inflation factor (VIF) screening and backward selection, pH, EC, OM, TN, and AHN were retained in the final RDA model. The significance of the RDA model and individual explanatory variables was tested using permutation tests. All bioinformatic and statistical analyses were performed by using QIIME2 v2024.5, R v4.4.2, and SPSS 23.0.

3 Results

3.1 The effects of DB-SR on local soil conditions and maize growth across sampling zones

Significant differences in soil physicochemical properties were observed among the sampling zones (Fig. 1a–c). Compared with SD, EC increased significantly in SN and SF by 77% and 45%, respectively ($P < 0.05$; Fig. 2a). In contrast, soil pH decreased significantly in SN and SF by 7% and 5%, respectively ($P < 0.05$; Fig. 2b). OM also decreased from SD to SN to SF, with reductions of 7% and 8% in SN and SF relative to SD, respectively ($P < 0.05$; Fig. 2c).

Maize growth differed significantly among the sampling zones (Fig. 2d–g). In detail, plant height was significantly ($P < 0.05$) greater in SN and SF than in SD. Stem diameter, shoot fresh weight, and shoot dry weight showed an increasing trend from SD to SN to SF, with significantly ($P < 0.05$) higher values in SF than in SD. Overall, maize growth was enhanced from SD to SN to SF under DB-SR.

3.2 Bacterial diversity and community composition across sampling zones

The Shannon index showed no significant differences among the SD, SN, and SF sampling zones in either bulk or rhizosphere soils based on one-way ANOVA ($P > 0.05$; Fig. 3a). Phylum-level compositional analysis displayed that the top 10 most abundant bacterial phyla were similar in bulk and rhizosphere soils, including Proteobacteria, Bacteroidetes, Actinobacteria, Acidobacteria, Firmicutes, Verrucomicrobia, Gemmatimonadetes, Planctomycetes, Chloroflexi, and Nitrospirae (Fig. 3b). Together,

these phyla accounted for 99.13% and 99.54% of the total bacterial sequences in bulk and rhizosphere soils, respectively. In bulk soil, the relative abundance of Chloroflexi was significantly ($P < 0.05$) higher in the SD and SN zones than in the SF zone. In rhizosphere soil, the relative abundances of Chloroflexi and Planctomycetes were significantly ($P < 0.05$) lower in SN than in SF, whereas the relative abundances of Cyanobacteria and Gemmatimonadetes were significantly ($P < 0.05$) higher in SD than in SF.

As shown by the RDA result based on bulk soil bacterial communities and corresponding bulk soil physicochemical properties (Fig. 3c), soil EC, pH, OM, TN, and AHN were retained in the final model after backward selection, while pH and AHN displayed strong correlation to the RDA1 axis in the ordination plot. As shown in Fig. 3d and e, NMDS based on Bray–Curtis dissimilarity showed that bacterial community composition differed significantly among sampling zones in bulk soil (PERMANOVA, $R^2 = 0.1118$, $P = 0.0110$), whereas no significant difference was detected among sampling zones in rhizosphere soil (PERMANOVA, $R^2 = 0.1052$, $P = 0.0870$).

3.3 Differentially abundant ASVs in bulk and rhizosphere soils and their association with maize growth traits

Differentially abundant ASVs among sampling zones were identified separately in bulk and rhizosphere soils using thresholds of FDR < 0.05 and $|\log_2$ fold change$| > 1$. As shown by Fig. 4a and b, pairwise comparisons using SF as the reference group in bulk soil, seven ASVs were enriched in SD compared to SF while four ASVs were enriched in SN compared to SF. In contrast, 32 ASVs were enriched in SF in comparisons with SD and SN. In rhizosphere soil, five and 12 ASVs were enriched in SD and SN relative to SF, respectively, whereas three ASVs were enriched in SF across comparisons with SD and SN.

The top 15 enriched ASVs in each soil compartment, ranked by overall abundance, were further examined. In bulk soil, *Shewanella*_ASV158, *Luteolibacter*_ASV185, *Salinimicrobium*_ASV434, and *Serratia*_ASV86 showed positive $\log_2$ fold changes in both comparisons, whereas the remaining ASVs showed negative $\log_2$ fold changes in both comparisons (Fig. 4c). In the rhizosphere, *Arthrobacter*_ASV266, *Sphingopyxis*_ASV89, and *Lysobacter*_ASV148 showed positive $\log_2$ fold changes in both comparisons. *Proteiniclasticum*_ASV713, *Pedobacter*_ASV268, and *Agrobacterium*_ASV14 showed positive $\log_2$ fold changes in SD vs SF but negative $\log_2$ fold changes in SN vs SF, whereas *Ochrobactrum*_ASV115, *Flavobacterium*_ASV95, *Sphingobacterium*_ASV70, and *Sphingobacterium*_ASV162 showed the opposite pattern. *Sphingobacterium*_ASV5, *Lutibacterium*_ASV126, *Phyllobacterium*_ASV150, *Thermomonas*_ASV98, and *Niabella*_ASV405 showed negative $\log_2$ fold changes in both comparisons (Fig. 4d).

Spearman's rank correlation analysis showed that several selected differential ASVs were significantly associated with shoot biomass traits. In bulk soil, *Alicyclobacillus*_ASV104, *Georgenia*_ASV330, *Clostridium*_ASV602, and *Clostridium*_ASV357 were significantly and positively correlated with both shoot fresh weight and shoot dry weight, and *Serpens*_ASV335 was significantly positively correlated only with shoot dry weight (Fig. 5a). Meanwhile, the *Thermomonas*_ASV98 and *Phyllobacterium*_ASV150

were significantly and positively correlated with both shoot fresh weight and shoot dry weight, and *Niabella*_ASV405 was significantly positively correlated only with shoot fresh weight in the rhizosphere (Fig. 5b).

3.4 Co-occurrence patterns of bacterial communities across sampling zones

Bacterial co-occurrence networks were compared among sampling zones in bulk and rhizosphere soils (Fig. 6). In bulk soil, network complexity, as reflected by node and edge numbers, increased from SD to SN and then decreased toward SF, with the highest complexity observed in SN (343 nodes and 644 edges; Fig. 6). The proportion of positive correlations decreased from 74.82% in SD to 66.46% in SN and 59.62% in SF, whereas modularity increased from 0.70 in SD to 0.76 in SN and 0.80 in SF (Fig. 6b). In rhizosphere soil, network complexity, as indicated by node and edge numbers, was lowest in SN (169 nodes and 256 edges; Fig. 6a). Overall, these results suggest that the ditch-centered spatial gradient under DB-SR had a stronger influence on bacterial association patterns in bulk soil than in rhizosphere soil.

4 Discussion

This study showed that DB-SR provided pronounced ditch-centered spatial heterogeneity in soda saline-alkali soils, accompanied by distinct contradictions in local soil conditions, maize growth, and bacterial community patterns. Soil pH, EC, and OM, as well as maize growth indicators, varied with distance from the straw-filled ditch, indicating that DB-SR reshaped the local soil environment and was associated with enhanced maize growth across zones. Taken together, our findings suggest that the effects of DB-SR in soda saline-alkali soils are reflected not only in localized improvement of soil conditions, but also in spatially differentiated enhancement of maize growth.

Previous findings have demonstrated that pH is an important factor in the amelioration of soda saline-alkali soils (Liu et al., 2026). In the present study, soil pH in SN and SF was significantly lower than that in SD, indicating that clear spatial differences in alkalinity formed among ditch-centered positions under DB-SR. It was reported that higher pH is often accompanied by reduced nutrient availability, Na^+ enrichment, soil particle dispersion, and decreased microbial activity in soda saline-alkali soils (Liu et al., 2026). Therefore, the lower pH in SN and SF suggests that the alkaline environment in these zones was alleviated to some extent. After deep straw burial, the ditch zone becomes a region where straw-derived organic matter is concentrated and decomposed (Kan et al., 2025). The release of CO_2 and low-molecular-weight organic acids during straw decomposition is widely reported (Jaillard et al., 2023), which may contribute to the local carbonate system and alleviate soil alkalinity. It is worth mentioning that the effect of straw decomposition on soil pH is also jointly regulated by processes such as water-salt migration and ion redistribution under field conditions (Yescas-Coronado et al., 2022).

Furthermore, soil OM and EC also varied with distance from the straw-filled ditch. The higher OM in the ditch zone was mainly related to straw input itself and to organic intermediate products released during decomposition (Li et al., 2025), suggesting that OM was more likely to accumulate where straw was buried in a concentrated manner. Changes in EC were related to increases or decreases in soluble ions in the soil solution. On the one hand, straw decomposition releases a certain amount of soluble organic substances and inorganic ions (Li et al., 2017). On the other hand, alterations in soil moisture, pore structure, and solute transport conditions in the ditch zone can also impact the local dissolution, movement, and redistribution of salts (Kan et al., 2025). Overall, DB-SR improved local soil conditions in some zones and reshaped physicochemical conditions across ditch-centered positions, thereby contributing to the enhanced maize growth observed away from the ditch center.

It is well known that the assembly of soil bacterial communities is mainly driven by soil environmental properties (Plassart et al., 2019; Jiao et al., 2015). Although the Shannon index did not differ significantly among sampling zones, community structure, differential ASVs, and co-occurrence relationships were all different in the current study, indicating that DB-SR altered the relative abundances of bacterial taxa and their potential interactions. RDA results showed that EC, pH, OM, TN, and AHN were associated with variation in community structure, suggesting that localized differences in salinity-alkalinity and nutrient status along the ditch gradient shaped bacterial community distribution. In line with previous findings (Sloan et al., 2007), the pattern of bacterial network in the current study was more pronounced in bulk soil, suggesting greater sensitivity to straw decomposition and local environmental variation, while rhizosphere soil remained relatively stable due to plant filtering effects. In addition, co-occurrence network analysis further showed that DB-SR reshaped potential association patterns among taxa, consistent with the observed changes in bacterial community composition, and this effect was stronger in bulk soil than in rhizosphere soil (Liu et al., 2025).

Several selected differential ASVs were significantly correlated with maize shoot fresh weight and shoot dry weight, suggesting that DB-SR-induced spatial heterogeneity may contribute to enhanced maize growth through its effects on specific bacterial taxa. Taxonomically, these significant differential ASVs in bulk soil mainly belonged to *Alicyclobacillus*, *Georgenia*, and *Clostridium*, whereas those in rhizosphere soil mainly belonged to *Phyllobacterium*, *Thermomonas*, and *Niabella*. *Alicyclobacillus* is commonly found in acidic or specialized environments (Ciuffreda et al., 2015), and its shifts may be related to local changes in pH and microhabitats after straw decomposition. *Georgenia* may likewise be associated with resource and environmental differences induced by DB-SR. *Clostridium* is associated with anaerobic decomposition of organic matter and can participate in carbohydrate transformation while producing metabolic products such as organic acids (Liberato et al., 2019). This leads to straw decomposition, nutrient release and thus indirectly promotes maize growth. In rhizosphere soil, *Phyllobacterium* is a common plant-associated bacterial genus, and some members can colonize the rhizosphere and exhibit potential growth-promoting effects (Mantelin et al., 2006). It was reported that the distributional change of *Thermomonas*, commonly found in soils and related environments (Wang et al., 2014), may be related to rhizosphere environmental shifts under DB-SR. Moreover, *Niabella* belongs to the *Bacteroidota* group, which is generally associated with organic substrate utilization (Ma et al., 2023), linking to rhizosphere

carbon-source inputs. Overall, the spatial distribution of these differential taxa indicates that DB-SR altered local environmental conditions and further influenced bacterial community composition, and such changes may indirectly affect maize growth.

This study was based on a single sampling time point and did not include a no-straw control. In addition, pretreatment baseline soil data were not available for the exact SD, SN, and SF positions before the establishment of DB-SR. Therefore, although the sampling zones were arranged within the same field and along replicated ditch-centered gradients, we cannot completely exclude the possibility that some differences in pH, EC, or nutrient status among zones partly reflected pre-existing spatial heterogeneity. Accordingly, the current conclusions mainly explain spatial heterogeneity and associations under DB-SR, but cannot yet fully reveal temporal dynamics, net DB-SR effects relative to conventional management, or definitive before–after changes. Future studies should include baseline measurements, no-straw controls, and continuous sampling across multiple crop stages to track dynamic changes in soil environment, microbial processes, and crop responses across ditch-centered positions.

5 Conclusion

In conclusion, DB-SR generated pronounced ditch-centered spatial heterogeneity in soda saline-alkali soils and was associated with enhanced maize growth. Under DB-SR, soil pH, EC, and OM differed significantly across the ditch-centered gradient, and these differences were associated with spatially differentiated maize growth. Meanwhile, DB-SR manipulated bacterial community composition and impacted co-occurrence network patterns, especially in bulk soil. Several differential ASVs assigned to taxa putatively associated with organic matter decomposition, carbon transformation, and plant growth promotion, including *Alicyclobacillus*, *Georgenia*, *Clostridium*, *Phyllobacterium*, *Thermomonas*, and *Niabella*, were observed to be correlated with maize shoot biomass traits. Overall, These results suggest that DB-SR may contribute to spatially improved maize performance by jointly shaping local soil conditions and bacterial communities, highlighting its potential application in soda saline-alkali farmland.

Abbreviations

DB-SR	Ditch-buried straw return
SD	Ditch zone
SN	Near-ditch zone
SF	Far-ditch zone
EC	Electrical conductivity
OM	Organic matter

AHN	Alkali-hydrolysable nitrogen
TN	Total nitrogen
AP	Available phosphorus
AK	Available potassium
ASVs	Amplicon sequence variants
NMDS	Non-metric multidimensional scaling
PERMANOVA	Permutational multivariate analysis of variance
FDR	False discovery rate
RDA	Redundancy analysis
VIF	Variance inflation factor
ANOVA	Analysis of variance
HSD	Honestly significant difference

Declarations

Ethics approval and consent to participate

No ethics approval was required for this study. The field experiment and collection of soil and maize (*Zea mays* L.) samples were conducted with permission from the landowner. The maize seeds used in this study were a commercially available cultivated variety, 'Tianyu 108', purchased from Jilin Yuntianhua Seed Industry Technology Co., Ltd., China, and were not collected from the wild. The maize straw used for ditch burial was collected from the preceding maize crop grown in the experimental field with permission from the landowner. This study complied with relevant institutional, national, and international guidelines and local legislation. No protected plant species or CITES-listed species were involved.

Consent for publication

Not applicable.

Competing interests

The authors have no relevant financial or non-financial interests to disclose.

Funding

This research was supported by the Chinese Academy of Sciences, the Fundamental Research Funds for the Central Universities (RENCAI2026011), and Jiangsu Qing Lan Project.

Author Contribution

Xuan Chen: Writing original draft, visualization, validation, software, resources. Paidamoyo N. Mataranyika: Reviewing, editing. Zhe Liu: Sampling, Measuring and data analysis. Tingting Li: reviewing, editing, funding acquisition. Pai Peng: Reviewing, editing. Xiaona Wei: reviewing, editing. Hongjun Liu: Reviewing, editing. Zhipeng Liu: Data curation, experimental design. Zongzhuan Shen: Supervising, writing, reviewing, editing, funding acquisition. Weiyu Shi: Supervising, reviewing, editing. Rong Li: Supervising, reviewing, editing.

Acknowledgements

Not applicable.

Data Availability

The raw 16S rRNA gene sequencing datasets supporting the conclusions of this article are available in the NCBI Sequence Read Archive repository, BioProject accession number PRJNA1490355, https://www.ncbi.nlm.nih.gov/bioproject/PRJNA1490355/.

References

1. Tarolli P, Luo J, Park E, Barcaccia G, Masin R. 2024. Soil salinization in agriculture: Mitigation and adaptation strategies combining nature-based solutions and bioengineering. *iScience* 27, 108830. https://doi.org/10.1016/j.isci.2024.108830
2. Wang G, Ni G, Feng G, Burrill HM, Li J, Zhang J, Zhang F. Saline-alkali soil reclamation and utilization in China: progress and prospects. Front Agricultural Sci Eng. 2024;11(2):216–28. https://doi.org/10.15302/j-fase-2024551.
3. Shan M, Wang C, Zhang Y, Yu Z, Fan Y, Bai A, Lu L, Ren L, Wu Y, Zhou W, Zhang M. Synergistic effect of the amendment on soybean yield increase and soil remediation in soda saline-alkali land: focusing on the soil quality index. Front Plant Sci. 2026;17:1818215. https://doi.org/10.3389/fpls.2026.1818215.
4. Shainberg I, Levy GJ. In: Wagenet RJ, Baveye P, Stewart BA, editors. Interacting Processes in Soil Science. *Advances in Soil Science*. Boca Raton, FL: Lewis; 1992. pp. 37–94. https://doi.org/10.1201/9781003070122.

5. Yu J, Wang Z, Meixner FX, Yang F, Wu H, Chen X. Biogeochemical characterizations and reclamation strategies of saline sodic soil in northeastern China. Clean Soil Air Water. 2010;38(10):1017–26. https://doi.org/10.1002/clen.201000276.
6. Pan L, Li R, Zhang Y, Li Q, Gao J, Yuan J. Effects of straw mulching on soil ecological stoichiometry characteristics and yield on sloping farmland in karst area, Southwestern China. Acta Ecol Sin. 2022;42(11):4428–38. https://doi.org/10.5846/stxb202104030867.
7. Dou S. A new model of straw enrichment and deep incorporation and engineering techniques. Acta Pedol Sin. 2019;56(3):553–60. https://doi.org/10.11766/trxb201809300331.
8. Kan ZR, Li Z, Amelung W, Zhang HL, Lal R, Bol R, Bian X, Liu J, Xue Y, Li FM, Yang H. Soil carbon accrual and crop production enhanced by sustainable subsoil management. Nat Geosci. 2025;18:631–8. https://doi.org/10.1038/s41561-025-01720-5.
9. Rengasamy P. Soil processes affecting crop production in salt affected soils. Funct Plant Biol. 2010;37:613–20. https://doi.org/10.1071/fp09249.
10. Zhao J, Ni T, Xun W, Huang X, Huang Q, Ran W, Shen B, Zhang R, Shen Q. Influence of straw incorporation with and without straw decomposer on soil bacterial community structure and function in a rice-wheat cropping system. Appl Microbiol Biotechnol. 2017;101:4761–73. https://doi.org/10.1007/s00253-017-8170-3.
11. Wu Z, Zhao Z, Lin W, Li J, Liu S, Zhou L, Luo Y, Liu J. Analysis of terminal restriction fragment length polymorphisms in soil bacterial communities in Chinese fir plantations that have undergone continuous cultivation. Acta Ecol Sin. 2019;39(19):7134–43. https://doi.org/10.5846/stxb201808041663.
12. Tang H, Xiao X, Li C, Tang W, Guo L, Wang K, Sun Y, Cheng K, Sun G, Pan X. Effects of recycling straw of different winter covering crops on rhizospheric microbial community functional diversity in a double-cropped paddy field. Acta Ecol Sin. 2018;38(18):6559–69. https://doi.org/10.5846/stxb201712162261.
13. Zhao D, Ling J, Wu G, Liu Z, Zhou S, Wen Y, Beule L. The incorporation of straw into the subsoil increases C, N, and P enzyme activities and nutrient supply by enriching distinctive functional microorganisms. Land Degrad Dev. 2023;34(5):1297–310. 10.1002/ldr.4533. https://onlinelibrary.wiley.com/doi/pdf/.
14. Cao Y, Ou Y, Lv N, Tao C, Liu H, Li R, Shen Z, Shen Q. Soil nutrient levels are associated with suppression of banana Fusarium wilt disease. Soil Ecol Lett. 2024;6(4):240247. https://doi.org/10.1007/s42832-024-0247-1.
15. Caporaso JG, Lauber CL, Walters WA, Berg-Lyons D, Lozupone CA, Turnbaugh PJ, Fierer N, Knight R. Global patterns of 16S rRNA diversity at a depth of millions of sequences per sample. Proc Natl Acad Sci USA. 2011;108:4516–22. 10.1186/s13059-019-1711-6. https://genomebiology.biomedcentral.com/track/pdf/.
16. Callahan BJ, McMurdie PJ, Rosen MJ, Han AW, Johnson AJA, Holmes SP. DADA2: High-resolution sample inference from Illumina amplicon data. Nat Methods. 2016;13(7):581–3.

https://doi.org/10.1038/nmeth.3869.

17. Werner JJ, Knights D, Garcia ML, Scalfone NB, Smith S, Yarasheski K et al. 2011. Bacterial Community Structures Are Unique and Resilient in Full-Scale Bioenergy Systems. *Proceedings of the National Academy of Sciences*, 108, 4158–4163. https://doi.org/10.1073/pnas.1015676108
18. Robinson MD, McCarthy DJ, Smyth GK. edgeR: a Bioconductor package for differential expression analysis of digital gene expression data. Bioinformatics. 2010;26(1):139–40. https://doi.org/10.1093/bioinformatics/btp616.
19. Yuan W, Yang D, Xu Z, Liu Y, Li X, Ding C, Wang Z. Diversity of soil microbial communities in the bulk and rhizosphere soils of Acanthopanax senticosus in different habitats. Curr Microbiol. 2025;82:73. https://doi.org/10.1007/s00284-024-04054-4.
20. Bastian M, Heymann S, Jacomy M. 2009. Gephi: An open source software for exploring and manipulating networks. *Proceedings of the International AAAI Conference on Web and Social Media*, 3(1), 361–362. https://doi.org/10.1609/icwsm.v3i1.13937
21. Langfelder P, Horvath S. WGCNA: an R package for weighted correlation network analysis. BMC Bioinformatics. 2008;9:559. https://doi.org/10.1186/1471-2105-9-559.
22. Csardi G, Nepusz T. 2006. The igraph software package for complex network research. InterJournal Complex Syst, 1695.
23. Liu RZ, Zhao XY, Wang LJ, Zhang X, Hu SP, Gao JL, Yu XF, Borjigin Q. Coupled effects of straw return practices on soil microbial functional potential and agricultural productivity in semi-arid region. Plant Soil. 2026;520:121–39. https://doi.org/10.1007/s11104-025-08186-9.
24. Ninkuu V, Liu Z, Qin A, Xie Y, Song X, Sun X. Impact of straw returning on soil ecology and crop yield: A review. Heliyon. 2025;11:e41651. https://doi.org/10.1016/j.heliyon.2025.e41651.
25. Wu J, Wang X, Chen K. Study on the straw-soil disturbance characteristics of a lift-type winged chisel plow. INMATEH - Agricultural Eng. 2025;76(2):394–403. https://doi.org/10.35633/inmateh-76-33.
26. Barrow NJ. Stimulated decomposition of soil organic matter during the decomposition of added organic materials. Aust J Agric Res. 1960;11:331–8. https://doi.org/10.1071/ar9600331.
27. Paul EA, Juma NG. Mineralization and immobilization of soil nitrogen by microorganisms. Ecological Bulletins No. 33: *Terrestrial Nitrogen Cycles: Processes, Ecosystem Strategies and Management Impacts*. Oikos Editorial Office; 1981. pp. 179–95. https://doi.org/10.2134/agronmonogr22.c6.
28. Adeleke R, Nwangburuka C, Oboirien B. Origins, roles and fate of organic acids in soils: A review. South Afr J Bot. 2017;108:393–406. https://doi.org/10.1016/j.sajb.2016.09.002.
29. Liao H, Hao X, Zhang Y, Qin F, Xu M, Cai P, Chen W, Huang Q. Soil aggregate modulates microbial ecological adaptations and community assemblies in agricultural soils. Soil Biol Biochem. 2022;172:108769. https://doi.org/10.1016/j.soilbio.2022.108769.
30. Ma H, Li P, Liu X, et al. Poly- Gamma- Glutamic Acid Enhanced the Drought Resistance of Maize by Improving Photosynthesis and Affecting the Rhizosphere Microbial Community. BMC Plant Biol. 2022;22:11. https://doi.org/10.1186/s12870-021-03392-w.

31. Wen T, Xie P, Penton CR, et al. Specific Metabolites Drive the Deterministic Assembly of Diseased Rhizosphere Microbiome Through Weakening Microbial Degradation of Autotoxin. Microbiome. 2022;10:177. https://doi.org/10.1186/s40168-022-01375-z.
32. Breemen Nvan. Effects of redox processes on soil acidity. Neth J Agric Sci. 1987;35(3):271–9. https://doi.org/10.18174/njas.v35i3.16724.
33. Zeng A, Hu W, Zhang L, Lin X, Zhang M, Zeng C. Effect of salinity and flood on the dissolved organic matter content and composition structure in the early stage of decomposition of Cyperus malaccensis litter. Acta Ecol Sin. 2020;40(8):2751–62. https://doi.org/10.5846/stxb201902250351.
34. Kaye JP, Hart SC. Competition for nitrogen between plants and soil microorganisms. Trends Ecol Evol. 1997;12(4):139–43. https://doi.org/10.1016/s0169-5347(97)01001-x.
35. Chalmandrier L, Müünkemüller T, Gallien L, de Bello F, Mazel F, Lavergne S, Thuiller W. A family of null models to distinguish between environmental filtering and biotic interactions in functional diversity patterns. J Veg Sci. 2013;24(5):853–64. https://europepmc.org/articles/pmc4003529?pdf=render.
36. Sloan WT, Woodcock S, Lunn M, Head IM, Curtis TP. Modeling taxa–abundance distributions in microbial communities using environmental sequence data. Microb Ecol. 2007;53:443–55. https://doi.org/10.1007/s00248-006-9141-x.
37. Wang Q, Cheng Y. Response of fine roots to soil nutrient spatial heterogeneity. Ying Yong Sheng Tai Xue Bao. 2004;15(6):1063–8.
38. Wang Y, Feng F, Ge J, Li Y, Yu X, et al. Effects and mechanisms of plant root exudates on soil remediation. Acta Ecol Sin. 2022;42(3):829–42. https://doi.org/10.5846/stxb202101030011.
39. Mauchline TH, Malone JG. Life in earth – the root microbiome to the rescue? Curr Opin Microbiol. 2017;37:23–8. https://doi.org/10.1016/j.mib.2017.03.005.
40. Keiluweit M, Nico PS, Kleber M, Fendorf S. Are oxygen limitations under recognized regulators of organic carbon turnover in upland soils? Biogeochemistry. 2016;127:157–71. https://doi.org/10.1007/s10533-015-0180-6.
41. Shi S, Nuccio EE, Shi ZJ, He ZL, Zhou JZ, Firestone MK. The interconnected rhizosphere: High network complexity dominates rhizosphere assemblages. Ecol Lett. 2016. https://doi.org/10.1111/ele.12630.
42. Nannipieri P, Ascher-Jenull J, Ceccherini MT, Pietramellara G, Renella G, Schloter M. Beyond microbial diversity for predicting soil functions: A mini review. Pedosphere. 2020;30(1):5–17. https://doi.org/10.1016/s1002-0160(19)60824-6.
43. Carr A, Diener C, Baliga NS, Gibbons SM. Use and abuse of correlation analyses in microbial ecology. ISME J. 2019;13:2647–55. https://doi.org/10.1038/s41396-019-0459-z.
44. Garayburu-Caruso VA, Stegen JC, Song H-S, Renteria L, Wells J, Garcia W, Resch CT, Goldman AE, Chu RK, Toyoda J, Graham EB. Carbon limitation leads to thermodynamic regulation of aerobic metabolism. Environ Sci Technol Lett. 2020;7(5):342–7. https://doi.org/10.1101/2020.01.15.905331.

45. Moran KK, Six J, Horwath WR, van Kessel C. Role of mineral-nitrogen in residue decomposition and stable soil organic matter formation. Soil Sci Soc Am J. 2005;69(4):648–60. https://doi.org/10.2136/sssaj2004.0301.
46. Liu X, Lin S, Li C, Ren S, Tang Y, Tang L, Zhang Z. Functional characteristics and distribution of microorganisms in saline and alkaline soils and their probiotic effects: a review. Microb Cell Fact. 2026;25:39. https://doi.org/10.1186/s12934-026-02926-x.
47. Jaillard B, Razanamalala K, Violle C, Bernard L. Nonlinear effects induced by interactions among functional groups of bacteria and fungi regulate the priming effect in Malagasy soils. Microorganisms. 2023;11:1106. https://doi.org/10.3390/microorganisms11051106.
48. Yescas-Coronado P, Segura-Castruita MA, Chávez-Rodríguez AM, Gómez-Leyva JF, Martínez-Sifuentes AR, Amador-Camacho O, González-Medina R. Covariables of Soil-Forming Factors and Their Influence on pH Distribution and Spatial Variability. Agriculture. 2022;12(12):2132. https://doi.org/10.3390/agriculture12122132.
49. Li Y, Guo L, Wu M, Li C. Effects of long-term conservation tillage on soil aggregate carbon fractions and microbial characteristics under rice-oilseed rape rotation systems. Appl Soil Ecol. 2025;206:105848. https://doi.org/10.1016/j.apsoil.2024.105848.
50. Li M, Zhang A, Wu H, Liu H, Lv J. Predicting potential release of dissolved organic matter from biochars derived from agricultural residues using fluorescence and ultraviolet absorbance. J Hazard Mater. 2017;334:86–92. https://doi.org/10.1016/j.jhazmat.2017.03.064.
51. Plassart P, Prévost-Bouré NC, Uroz S, Dequiedt S, Stone D, et al. Soil parameters, land use, and geographical distance drive soil bacterial communities along a European transect. Sci Rep. 2019;9:605. https://doi.org/10.1038/s41598-018-36867-2.
52. Jiao J, Wang J, Huang Y. Bacterial community features are shaped by geographic location, physicochemical properties, and oil contamination of soil in main oil fields of China. Microb Ecol. 2015;70:265–76. https://doi.org/10.1007/s00248-015-0572-0.
53. Liu Y, Zhou H, Xu G, Zhang Q, Liu X. Bacterial community structure in bulk soil and rhizosphere of alpine plants exhibits opposite longitudinal patterns. Basic Appl Ecol. 2025;86:11–20. https://doi.org/10.1016/j.baae.2025.04.008.
54. Ciuffreda E, Bevilacqua A, Sinigaglia M, Corbo MR. Alicyclobacillus spp.: New insights on ecology and preserving food quality through new approaches. Microorganisms. 2015;3(4):625–40. https://doi.org/10.3390/microorganisms3040625.
55. Liberato V, Benevenuti C, Coelho F, Botelho A, Amaral P, Pereira N Jr., Ferreira T. Clostridium sp. as bio-catalyst for fuels and chemicals production in a biorefinery context. Catalysts. 2019;9(11):962. https://doi.org/10.3390/catal9110962.
56. Mantelin S, Desbrosses G, Larcher M, Tranbarger TJ, Cleyet-Marel J-C, Touraine B. Nitrate-dependent control of root architecture and N nutrition are altered by a plant growth-promoting Phyllobacterium sp. Planta. 2006;223:591–603.

57. Wang L, Zheng S, Wang D, Wang L, Wang G. Thermomonas carbonis sp. nov., isolated from the soil of a coal mine. Int J Syst Evol MicroBiol. 2014;64:3631–5. https://doi.org/10.1099/ijs.0.063800-0.
58. Ma K, Ye Y, Fu Y, Fu G, Sun C, Xu X. Genomic and phylotypic properties of three novel marine Bacteroidota from bare tidal flats reveal insights into their potential of polysaccharide metabolism. Front Mar Sci. 2023;10:1222157. https://doi.org/10.3389/fmars.2023.1222157.

Figures

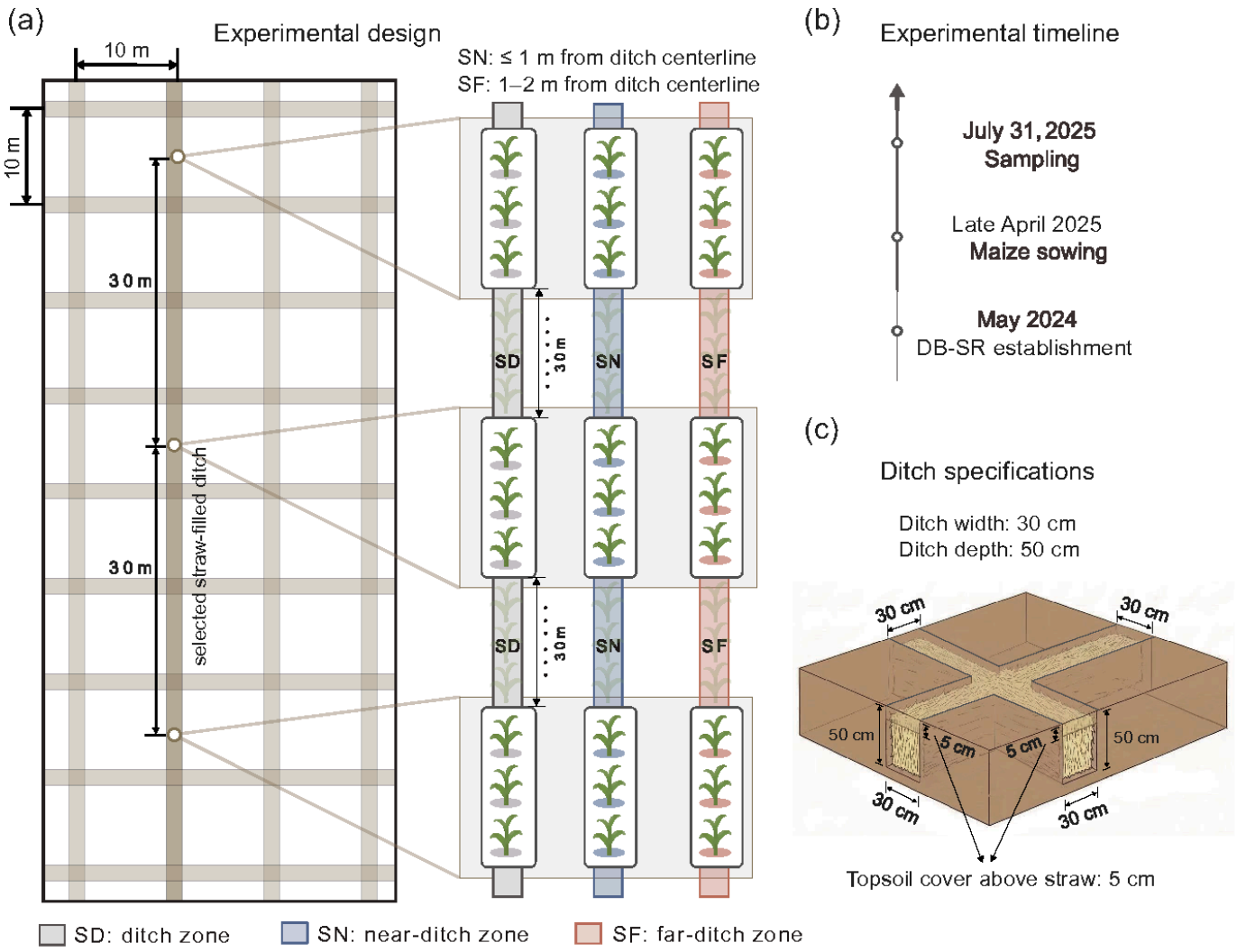


Figure 1

Experimental design and sampling scheme of the field study. (a) Schematic diagram of the field layout showing straw-filled ditches arranged in a 10 m × 10 m grid, a selected straw-filled ditch for sampling, three sampling sites at 30-m intervals, and three sampling zones defined according to horizontal

distance from the ditch centerline: SD, ditch zone; SN, near-ditch zone; and SF, far-ditch zone. (b) Experimental timeline showing ditch-buried straw return (DB-SR) establishment in May 2024, maize sowing in late April 2025, and sampling on July 31, 2025. (c) Ditch specifications: 30 cm in width, 50 cm in depth, and 5 cm in topsoil cover.

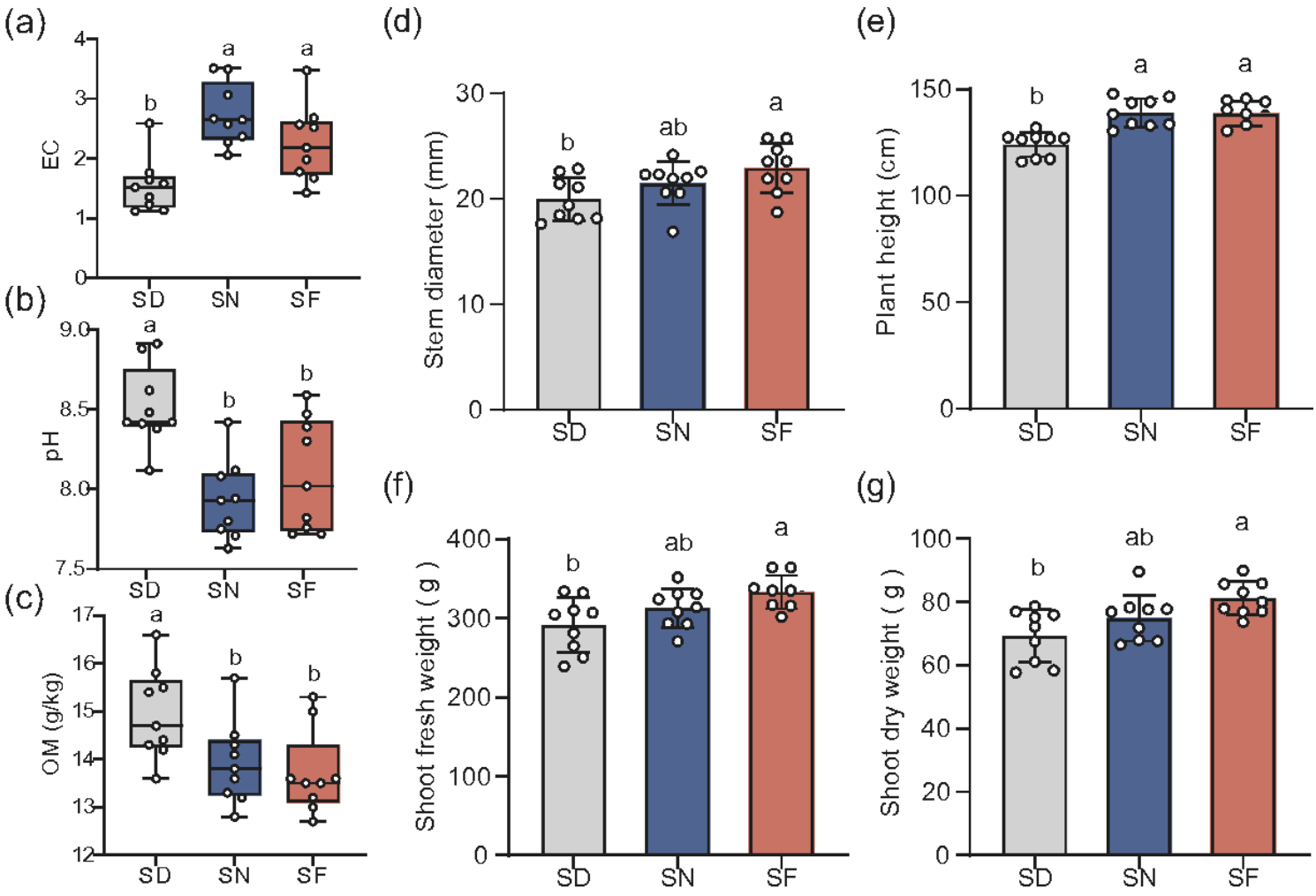


Figure 2

Straw ditch burial altered soil physicochemical properties and improved maize growth across sampling zones. (a) EC across the three sampling zones. (b) pH across the three sampling zones. (c) OM across the three sampling zones. (d) Stem diameter across the three sampling zones. (e) Plant height across the three sampling zones. (f) Shoot fresh weight across the three sampling zones. (g) Shoot dry weight across the three sampling zones. Boxplots show the distribution of soil physicochemical property values in each sampling zone, with points indicating individual observations (n = 9). Bars represent mean values of maize growth traits, with points indicating individual plant measurements (n = 9), and error bars represent standard errors. Different letters above the boxes or bars indicate significant differences among sampling zones ($P < 0.05$) based on one-way ANOVA followed by Tukey's HSD test.

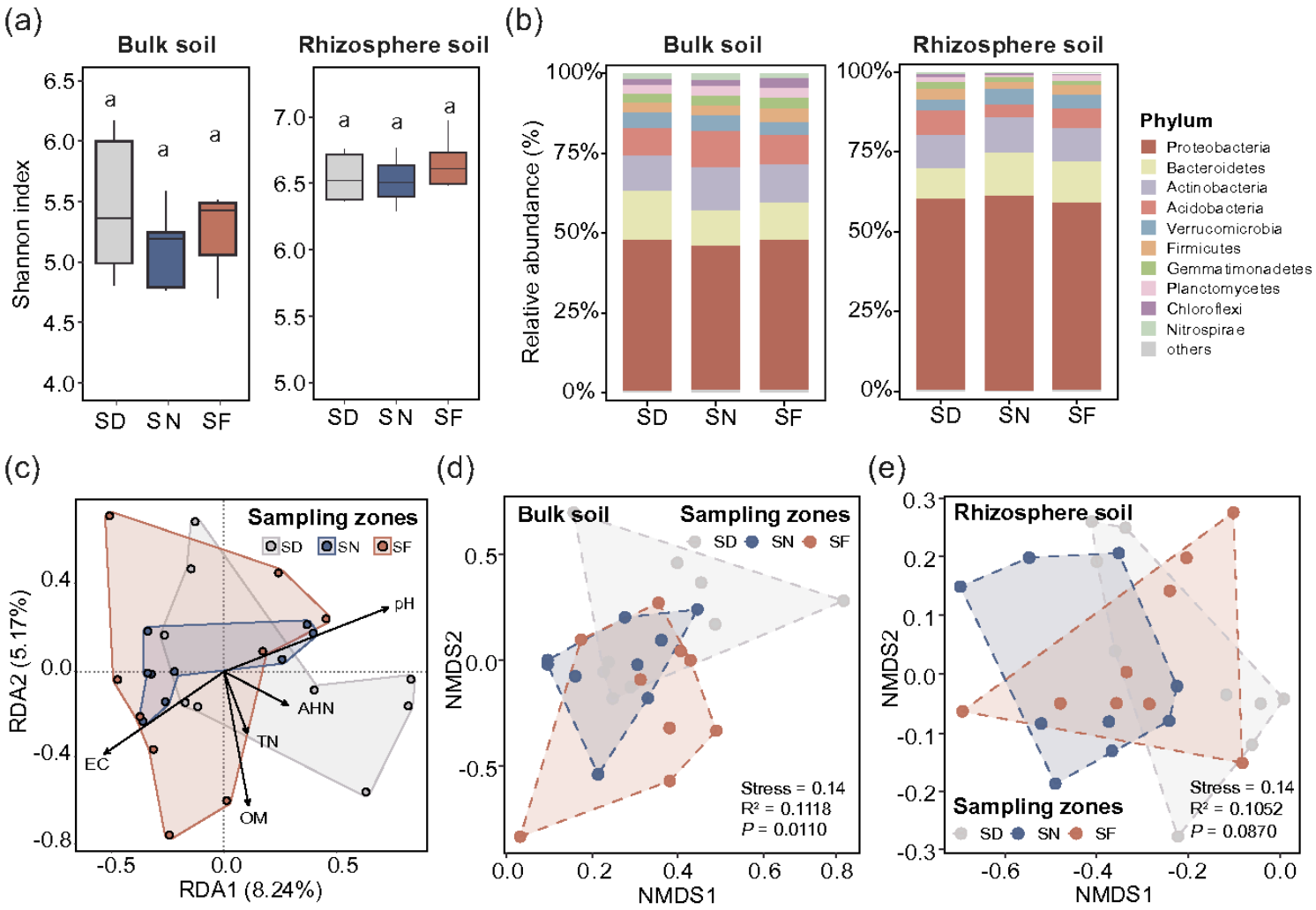


Figure 3

Bacterial diversity, community composition, and community structure across sampling zones in bulk and rhizosphere soils. (a) Shannon diversity index of bacterial communities in bulk and rhizosphere soils across the three sampling zones (SD, SN, and SF). (b) Relative abundance of the ten most abundant bacterial phyla in bulk and rhizosphere soils across the three sampling zones. Phyla with a mean relative abundance <1% were grouped as “others”. (c) Redundancy analysis (RDA) of bulk soil bacterial communities and corresponding bulk soil physicochemical properties. (d–e) Non-metric multidimensional scaling (NMDS) plots based on Bray–Curtis dissimilarity for bacterial communities in bulk (d) and rhizosphere (e) soils. Points represent samples, and shaded polygons indicate 95% confidence intervals. Stress values, PERMANOVA R^2, and *P* values are shown in the panels.

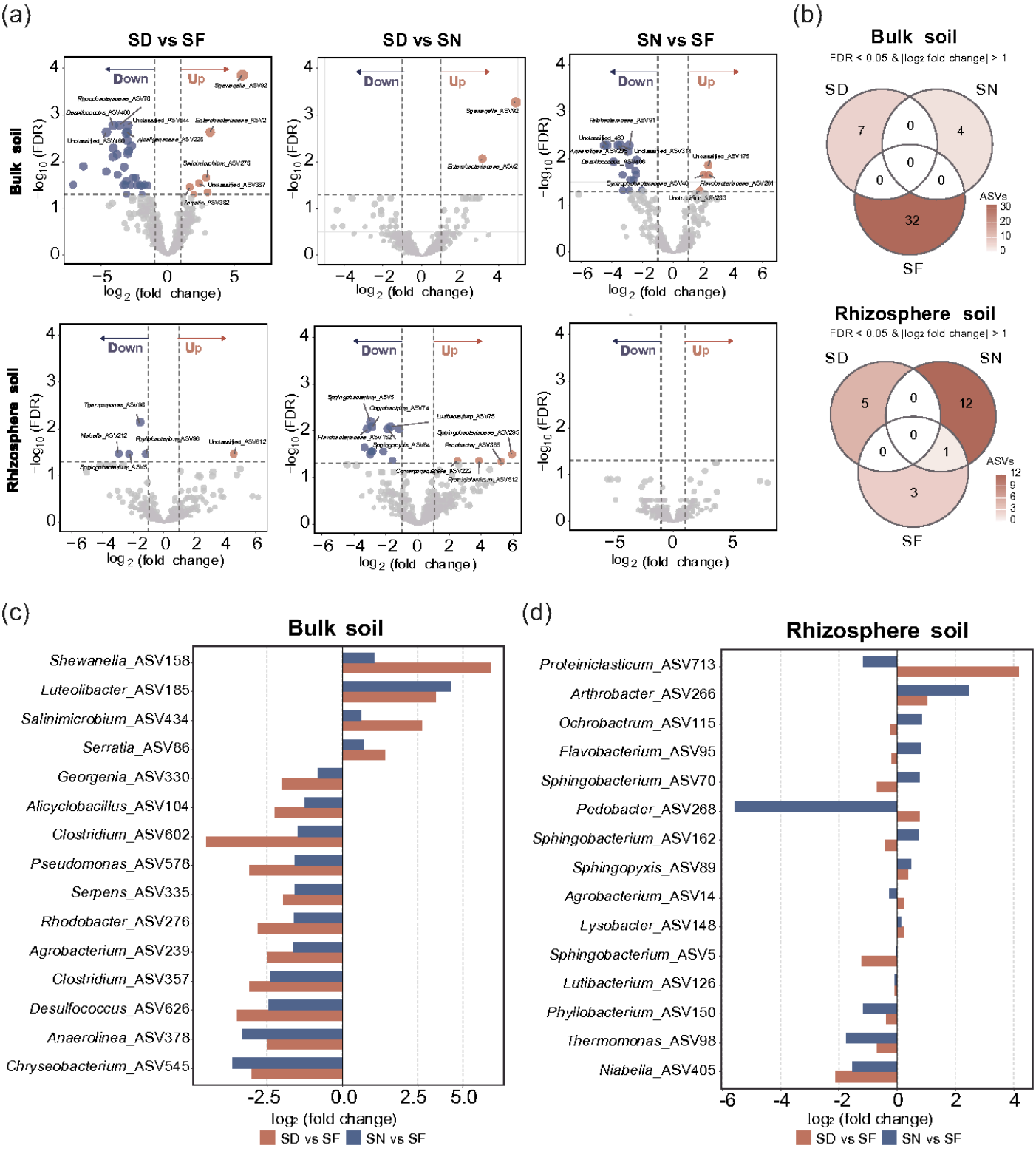


Figure 4

Differentially abundant ASVs across sampling zones in bulk and rhizosphere soils. (a) ASVs with FDR < 0.05 and $|\log_2$ fold change$| > 1$ were considered significant, and the top five ASVs on each side were labeled, ranked by FDR. (b) Venn diagrams showing the overlaps among ASVs enriched in SD, SN, and SF in bulk and rhizosphere soils. (c) Bar plot of $\log_2$ fold changes for the 15 most abundant ASVs enriched

in bulk soil from the SD vs SF and SN vs SF comparisons. (d) Bar plot of log_2 fold changes for the 15 most abundant ASVs enriched in rhizosphere soil from the SD vs SF and SN vs SF comparisons.

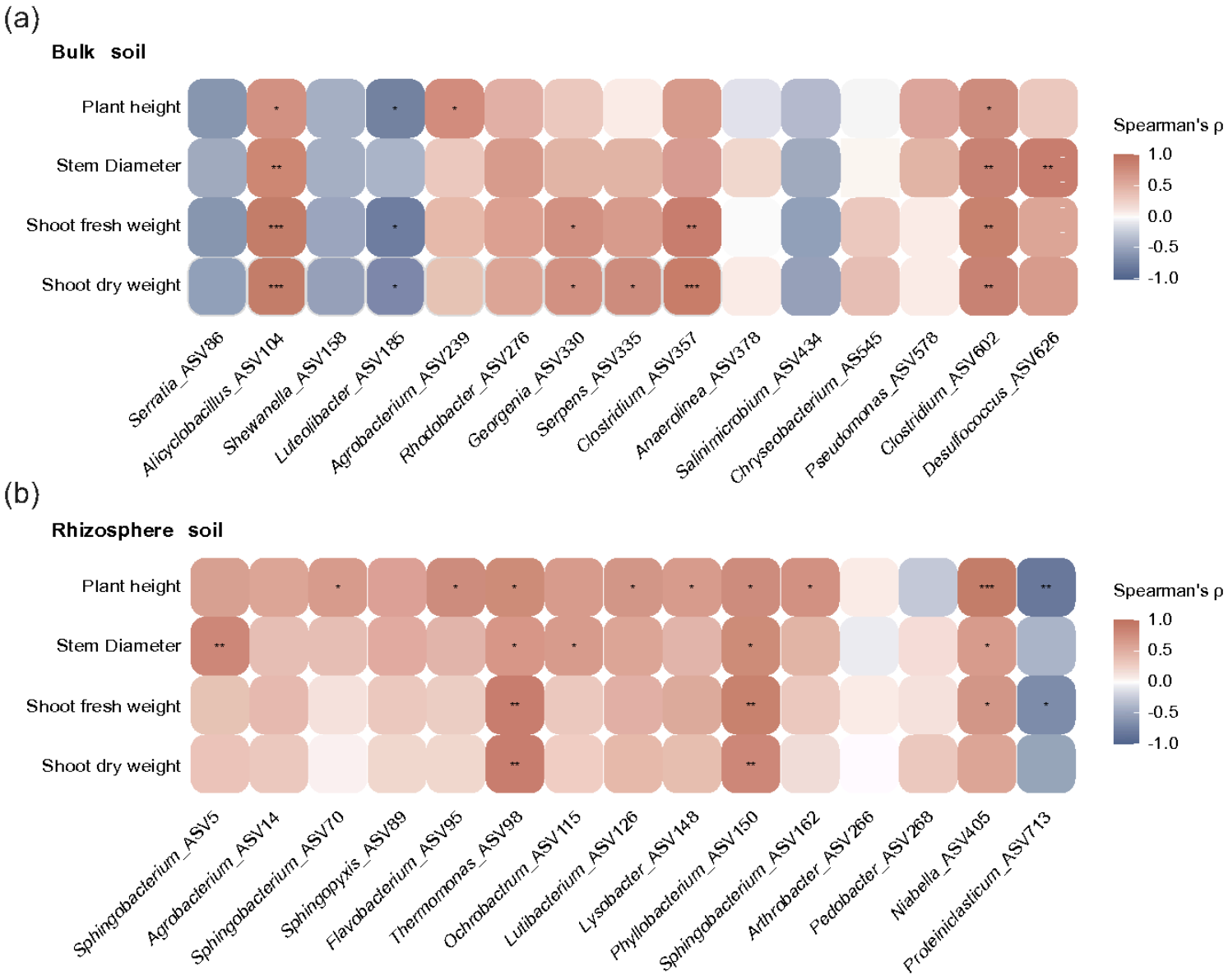


Figure 5

Spearman correlations between plant growth traits and enriched ASVs in bulk and rhizosphere soils. (a) Heatmap of Spearman correlations between plant growth traits and enriched ASVs in bulk soil. (b) Heatmap of Spearman correlations between plant growth traits and enriched ASVs in rhizosphere soil. Color indicates Spearman's correlation coefficient (ρ), and asterisks denote significance levels (*P < 0.05, **P < 0.01, ***P< 0.001).

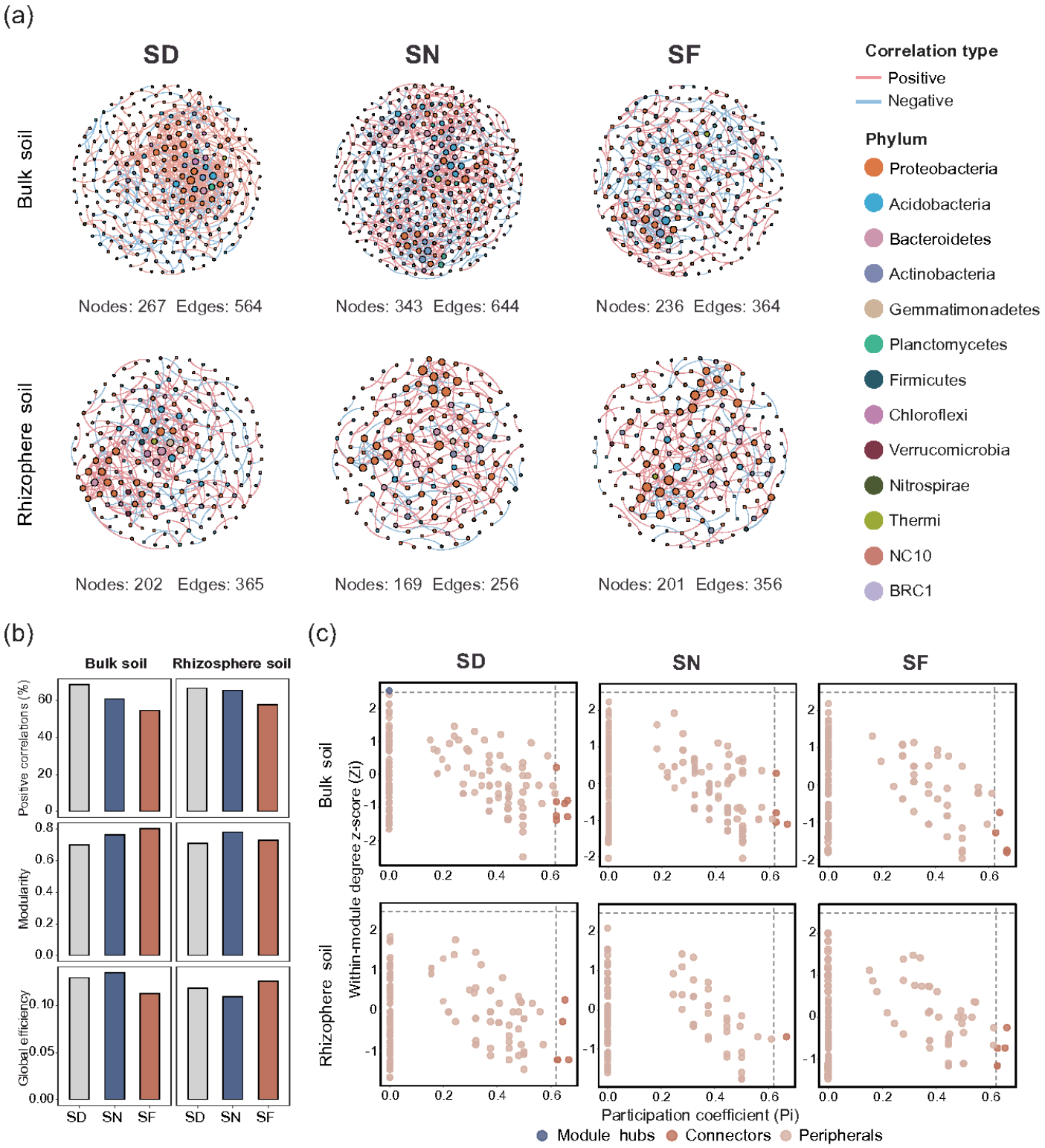


Figure 6

Bacterial co-occurrence networks and node roles in bulk and rhizosphere soils across zones. (a) Co-occurrence networks of core bacterial ASVs in bulk and rhizosphere soils from the straw-ditch zone (SD), near-ditch zone (SN), and far-ditch zone (SF). (b) Topological properties of the networks, including the proportion of positive correlations, modularity, and global efficiency. (c) Zi–Pi plots showing node topological roles. Dashed lines indicate the thresholds used for classification. Core ASVs were defined

as those detected in all nine biological replicates within each group. Nodes represent ASVs and are colored by phylum. Edges indicate significant Spearman's rank correlations ($|\rho| \geq 0.85$, $P < 0.05$), with pink and blue lines representing positive and negative correlations, respectively. The numbers of nodes and edges are shown for each network.